

Supporting Information

Enhanced photocatalytic activity of BiVO₄ coupled with iron-based complexes for water oxidation under visible light irradiation

Xiangming Liang^a, Junqi Lin^a, Xiaohu Cao^a, Wanjun Sun^a, Junyi Yang^a, Baochun Ma^{a*} and Yong Ding^{a,b*}

^a *State Key Laboratory of Applied Organic Chemistry, Key Laboratory of Nonferrous Metal Chemistry and Resources Utilization of Gansu Province, College of Chemistry and Chemical Engineering, Lanzhou University, Lanzhou 730000, China. E-mail: dingyong1@lzu.edu.cn*

^b *State Key Laboratory for Oxo Synthesis and Selective Oxidation, Lanzhou Institute of Chemical Physics, Chinese Academy of Sciences, Lanzhou 730000, China*

* To whom correspondence should be addressed.

E-mail addresses: mabaochun@lzu.edu.cn; dingyong1@lzu.edu.cn

Oxygen evolution yield (O₂ yield) calculation

The oxygen evolution yield (O₂ yield) were determined for the photocatalytic water oxidation under the following conditions: 100 mW/cm² under illumination at 420 nm; 25 µM Fe complexes, 50.0 mg BiVO₄, 5.0 mM NaIO₃, 15 mL acetate buffer (0.2 M, pH=4.0); total reaction volume is 15 mL and overall volume is ~32 mL; vigorous agitation using a magnetic stirrer.

Pure BiVO₄ system (reaction time is 20 h):

$$\begin{aligned}\text{O}_2 \text{ yield} &= \frac{\text{mole of detected O}_2 \text{ evolution}}{\text{mole of theoretic O}_2 \text{ evolution}} \times 100\% \\ &= 4 \times \frac{\text{mole of O}_2 \text{ evolution}}{6 \times \text{mole of NaIO}_3} \times 100\% \\ &= 4 \times \frac{14.4 \mu\text{mol}}{6 \times 5 \text{ mM} \times 15 \text{ ml}} \times 100\% \\ &= 12.8\%\end{aligned}$$

Addition complex 2 into BiVO₄ system (reaction time is 20 h):

$$\begin{aligned}\text{O}_2 \text{ yield} &= \frac{\text{mole of detected O}_2 \text{ evolution}}{\text{mole of theoretic O}_2 \text{ evolution}} \times 100\% \\ &= 4 \times \frac{\text{mole of O}_2 \text{ evolution}}{6 \times \text{mole of NaIO}_3} \times 100\% \\ &= 4 \times \frac{111.5 \mu\text{mol}}{6 \times 5 \text{ mM} \times 15 \text{ ml}} \times 100\% \\ &= 99.1\%\end{aligned}$$

Apparent quantum efficiency (AQE)

The apparent quantum efficiency (AQE) was calculated from the ration of the number of reacted electrons during oxygen evolution (equivalent to n_{O₂}) to the number of incident photons n_p as following, where t is the irradiation time (s), S is the effective light irradiation area (m²), and Q is the photon flux of the incident light (µmol (photons) m⁻² s⁻¹).

Addition Fe complexes into BiVO₄ system:

$$n_p = t \times S \times Q = 3600 \text{ s} \times \pi \times 0.015 \times 0.0125 \times 46 \mu\text{mol m}^{-2} \text{ s}^{-1} = 97.497 \mu\text{mol}$$

$$\begin{aligned}\text{AQE} &= \frac{\text{number of reacted electrons}}{\text{number of incident photons}} \times 100\% \\ &= \frac{4 \times n_{\text{O}_2}}{n_p} \times 100\% \\ &= \frac{4 \times 10.8}{97.497} \times 100\%\end{aligned}$$

$$= 44.3 \%$$

Pure BiVO₄ system:

$$n_p = t \times S \times Q = 3600 \text{ s} \times \pi \times 0.015 \times 0.0125 \times 46 \mu\text{mol m}^{-2} \text{ s}^{-1} = 97.497 \mu\text{mol}$$

$$\begin{aligned} \text{AQE} &= \frac{\text{number of reacted electrons}}{\text{number of incident photons}} \times 100\% \\ &= \frac{4 \times n_{\text{O}_2}}{n_p} \times 100\% \\ &= \frac{4 \times 1.1}{97.497} \times 100\% \\ &= 4.5 \% \end{aligned}$$

Ligand Synthesis.

The synthesis of ligand TPA has been reported previously.¹ To a mixture of 3.12 g (14.7 mmol) of sodium triacetoxyborohydride 0.54 g (5.26 mmol) of 2-(aminomethyl)pyridine stirring in CH₂Cl₂ (75 mL) was added 1.00 mL (10.5 mmol) of pyridine-2-carboxaldehyde. Upon completion of addition, stirring was continued for a further 18 h. Subsequently, a saturated aqueous sodium hydrogen carbonate solution was added, and after 15 min of stirring, an extraction of the mixture using ethyl acetate was performed. The organic fraction was dried (Na₂SO₄), and the solvent removed. The residue was extracted several times with small quantities of petroleum ether; the extracts were combined and the solvent removed to give TPA as a yellow solid (1.1 g, 72.1 % yield).

The synthesis of the ligand H-mpaq.² To a CH₃CN solution (50 mL) of 8-aminoquinoline (2.5 g, 17.4 mmol) and Na₂CO₃ (2.2 g, 20.8 mmol), bromoacetyl bromide (4.2 g 20.8 mmol) was slowly added under N₂, and the resulting mixture was stirred for 4.5 h at 0 °C. After removal of Na₂CO₃ through a Celite 545 pad, the filtrate was evaporated *in vacuo* to obtain a pale pink powder. The resulting powder was dissolved in CH₃CN (50 mL), to which Na₂CO₃ (1.2 g, 11.4 mol) and *N*-methyl-*N*-(2-pyridylmethyl)amine (1.1 g, 9.0 mmol) were added under N₂. The mixture was stirred overnight at 0 °C. After removal of Na₂CO₃ by a Celite 545 pad, the filtrate was evaporated *in vacuo* to obtain a viscous yellow oil. The crude product was purified by a column chromatography (Al₂O₃, hexane/ethyl acetate (1/1) to ethyl acetate as eluent). The product was obtained as a yellowish white solid (1.2 g, 41.1% yield).

The synthesis of the ligand N4Py.³ Picolyl chloride hydrochloride (6.8 g, 41.5 mmol) was added to an aqueous solution of NaOH (5M, 8.3 mL) at 0°C. After stirring for 10 min, this solution was added to bis(2-pyridyl)methylamine (4.13 g, 20.8 mmol) and another portion of aqueous NaOH (5 M, 8.3 mL). This solution was allowed to stir for 48 h at 25 °C. and then concentrated HClO₄ was added to precipitate a yellow solid. which was recrystallized from hot water. Treatment of this perchlorate salt with 2.5 M NaOH solution and extraction with dichloromethane yielded the free amine of N4Py (2.8 g, 37.2% yield).

Complex Synthesis

The synthesis of the $[(\text{TPA})\text{Fe}(\text{Cl})_2]\text{Cl}$ (**1**).¹ A solution of TPA (200 mg, 0.69 mmol) in 2 mL of MeCN was added to a suspension of FeCl_3 (112 mg, 0.69 mmol) in 5 mL of MeCN to produce a reddish suspension. After stirring at room temperature for 1 hour, the reaction mixture was filtered to yield a light red solution. Et_2O was added to the filtrate to precipitate the compound as a yellow powder (193 mg, 62% yield). FT-IR spectrum: 1606(S), 1485(m), 1443(s), 1289(m), 1159(m), 1097(m), 1054(m), 1025(s), 910(w), 817(w), 765(s), 731(m). Elemental analysis calculated (%) for $\text{C}_{18}\text{H}_{18}\text{Cl}_3\text{FeN}_4$: C, 47.77; H, 4.01; N, 12.38. Found: C, 48.37; H, 4.25; N, 12.70. ESI-MS. Found: 416.04. $[\text{FeTPACl}_2]^+$, $\text{C}_{18}\text{H}_{18}\text{Cl}_2\text{FeN}_4^+$, m/z 416.03.

The synthesis of the $[\text{Fe}_2(\text{TPA})_2(\mu\text{-O})\text{Cl}_2]\text{Cl}_2$ (**2**).¹ TPA (0.145 mg, 0.5 mmol) was dissolved in 20 mL of MeOH and treated with Et_3N (0.31 mL, 2.25 mmol). $\text{FeCl}_3 \cdot 6\text{H}_2\text{O}$ (0.135 g, 0.5 mmol) in a small volume (1-2 mL) of MeOH was added to the resulting solution of TPA. To this resultant red solution was added NaOAc (0.034 g, 0.25 mmol). FT-IR spectrum: 1605 (s), 1571 (m), 1485 (m), 1295 (m), 1100 (m), 1053 (m), 1024 (m), 957 (w), 827 (s), 766 (s), 624 (m). Elemental analysis calculated (%) for $\text{C}_{36}\text{H}_{36}\text{Cl}_4\text{Fe}_2\text{N}_8\text{O}$: C, 48.79; H, 4.55; N, 12.64; Found: C, 48.67; H, 4.55; N, 12.70. ESI-MS. Found: 813.11; $[\text{Fe}_2\text{TPA}_2(\mu\text{-O})\text{Cl}_3]^+$, $\text{C}_{36}\text{H}_{36}\text{Cl}_3\text{Fe}_2\text{N}_8\text{O}^+$, m/z 813.08.

The synthesis of the $\text{Fe}(\text{mpaq})\text{Cl}_2$ (**3**).² To a solution of H-mpaq (200 mg, 0.65 mmol) in CH_3OH (2 mL) in a glass vial, Et_3N (91 μL , 0.65 mmol) and a solution of FeCl_3 (130 mg, 0.78 mmol) in CH_3OH (2 mL) were slowly added. The dark green mixture was stirred for 3 hours. The precipitated green crystals were collected by filtration, washed with CH_3OH , and dried in vacuo. The products was isolated as a dark green powder; 240 mg (81% yield). FT-IR spectrum: 1629 (s), 1590 (m), 1573 (m), 1503 (m), 1467 (m), 1387 (s), 1356 (m), 1328 (m), 1306 (m), 1237 (m), 1103 (m), 1022 (m), 966 (m), 824 (m), 783 (m), 770 (m), 758 (m). UV-vis (CH_3CN): 615 nm, 360 nm. Elemental analysis calculated (%) for $\text{C}_{18}\text{H}_{19}\text{Cl}_2\text{FeN}_4\text{O}_2$: C, 48.03; H, 4.25; N, 12.45. Found: C, 48.03; H, 4.02; N, 12.09. ESI-MS. Found: 395.96. $[\text{Fe}(\text{mpaq})\text{Cl}]^+$, $\text{C}_{18}\text{H}_{17}\text{ClFeN}_4\text{O}^+$, m/z 396.04.

The synthesis of the $[\text{Fe}(\text{N4Py})(\text{CH}_3\text{CN})](\text{ClO}_4)_2$ (**4**).⁴ $\text{Fe}(\text{ClO}_4)_2 \cdot 10\text{H}_2\text{O}$ (0.215 g, 0.403 mmol) has added to a solution of N4Py (0.144 g, 0.392 mmol) in methanol:acetonitrile (1: 1) . The solution was allowed to stir for 5 min. and then was placed in a n ethyl acetate bath The red

crystalline product was collected and washed with ethyl acetate to yield **1** as dark red crystals (0.179 g, 65 % yield). FT-IR spectrum: 1605 (m), 1464 (s), 1447 (m), 1158 (m), 1093 (vs), 914 (m), 765 (s), 624 (s). UV-Vis (acetone): 382, 458. Elemental analysis calculated (%) for $C_{25}H_{28}Cl_2FeN_6O_{10}$: C, 42.94; H, 4.04; N, 12.02; Found: C, 43.21; H, 3.76; N, 12.02. ESI-MS. Found: 211.56. $[Fe(N4Py)]^{2+}$, $C_{23}H_{21}FeN_5^{2+}$, m/z 211.56.

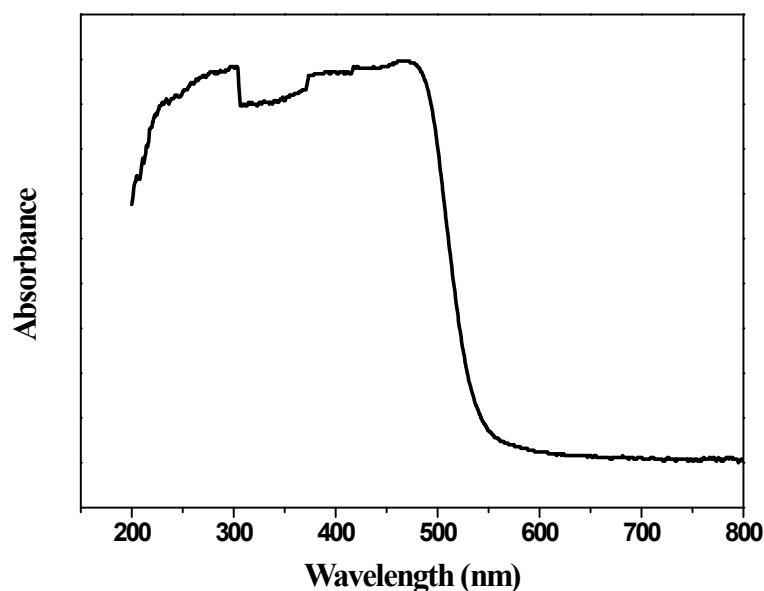


Fig. S1. UV-vis diffuse reflectance spectrum of $BiVO_4$.

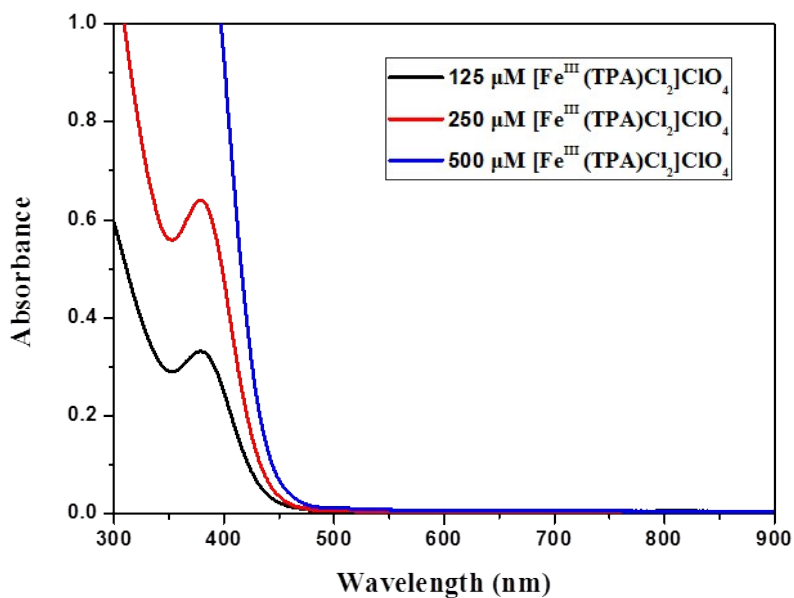


Fig. S2 UV-vis spectra for **1** at different concentrations: 125, 250, and 500 μM in an aqueous solution.

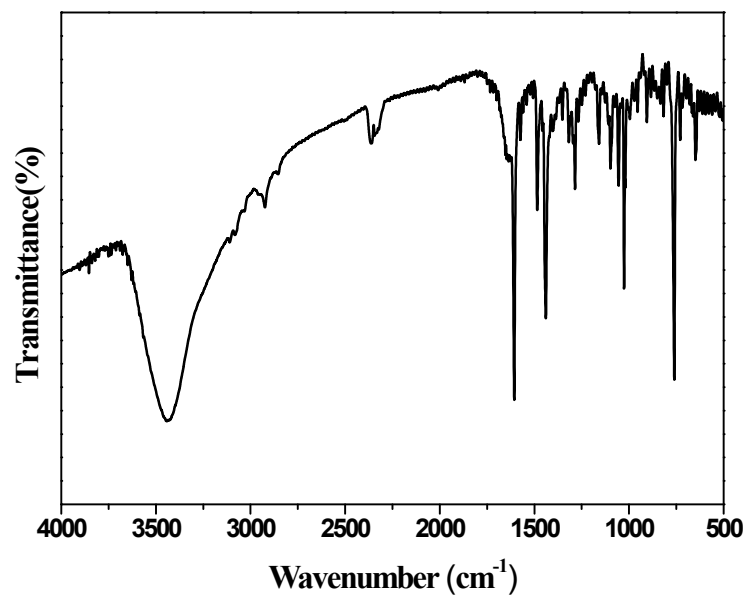


Fig. S3 FT-IR spectrum of **1** (cm^{-1}): 1606(s), 1485(m), 1443(s), 1289(m), 1159(m), 1097(m), 1054(m), 1025(s), 910(w), 817(w), 765(s), 731(m).

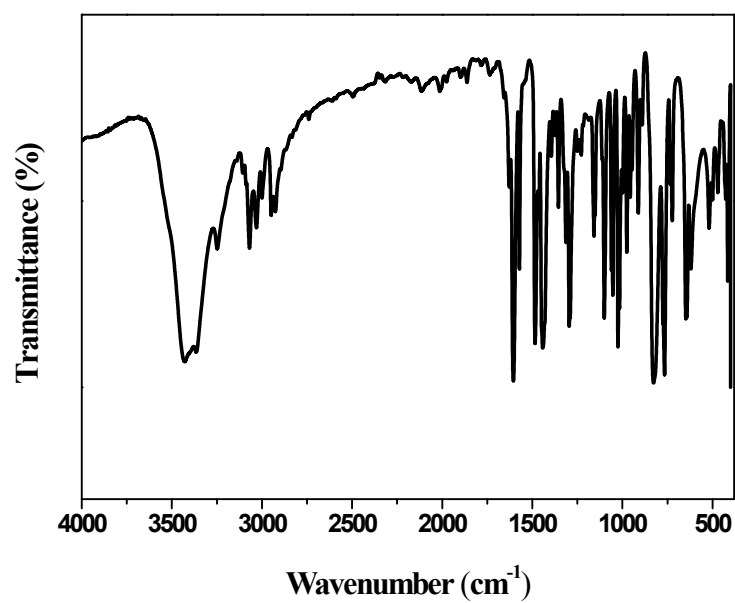


Fig. S4 FT-IR spectrum of **2** (cm^{-1}): 1605 (s), 1571 (m), 1485 (m), 1295 (m), 1100 (m), 1053 (m), 1024 (m), 957 (w), 827 (s), 766 (s), 624 (m).

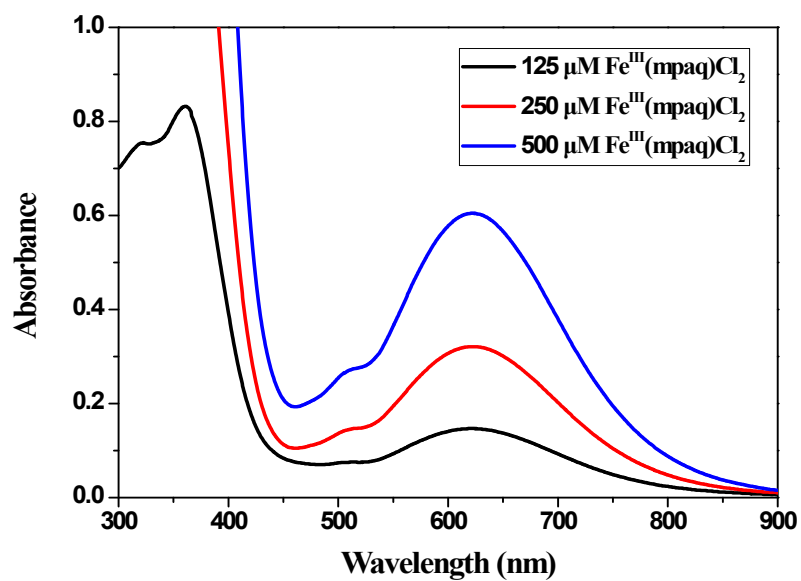


Fig. S5 UV-vis spectra for **3** at different concentrations: 125, 250, and 500 μM in CH_3CN .

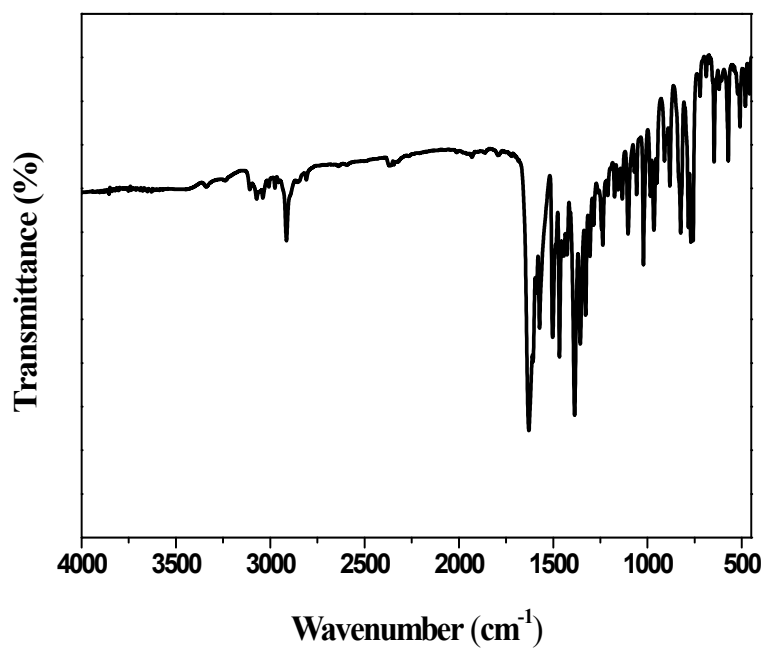


Fig. S6 FT-IR spectrum of **3** (cm^{-1}): 1629 (s), 1590 (m), 1573 (m), 1503 (m), 1467 (m), 1387 (s), 1356 (m), 1328 (m), 1306 (m), 1237 (m), 1103 (m), 1022 (m), 966 (m), 824 (m), 783 (m), 770 (m), 758 (m).

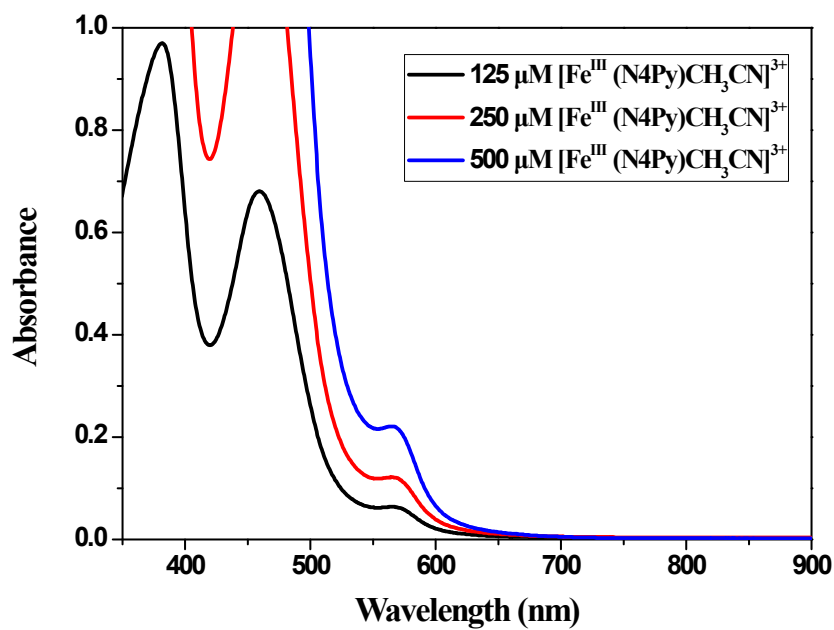


Fig. S7 UV-vis spectra for **4** at different concentrations: 125, 250, and 500 μM in MeOH.

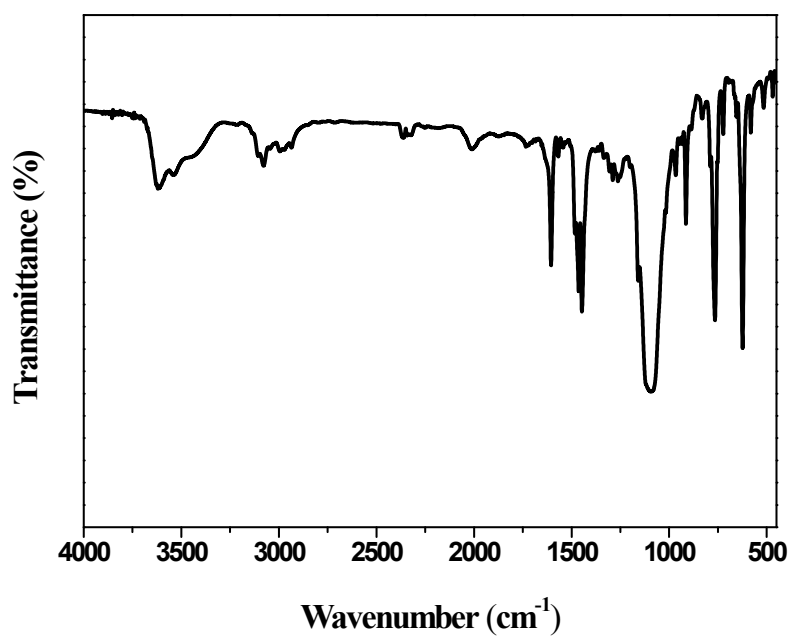


Fig. S8 FT-IR spectrum of **4** (cm^{-1}): 1605 (m), 1464 (s), 1447 (m), 1158 (m), 1093 (vs), 914 (m), 765 (s), 624 (s).

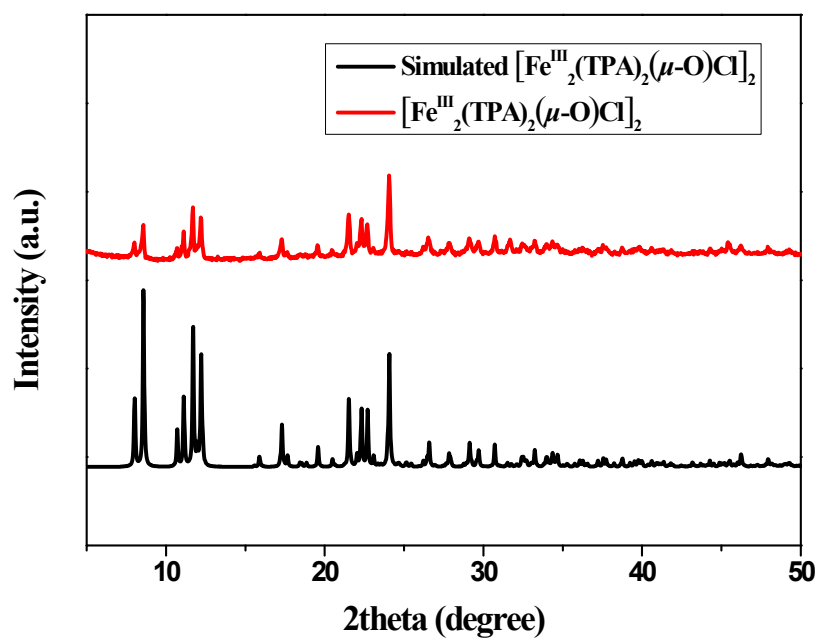


Fig. S9 Measured (red) and simulated (black) powder X-ray diffraction data of **2**.

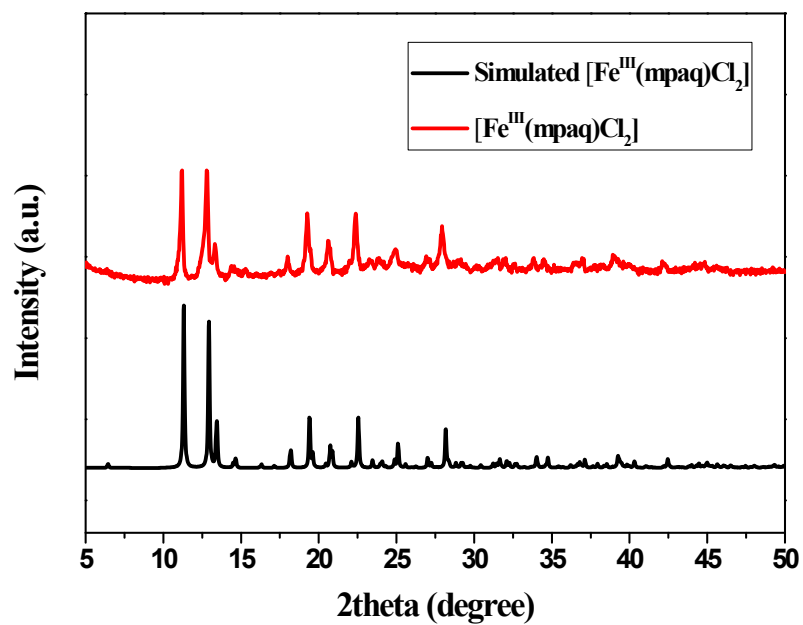


Fig. S10 Measured (red) and simulated (black) powder X-ray diffraction data of **3**.

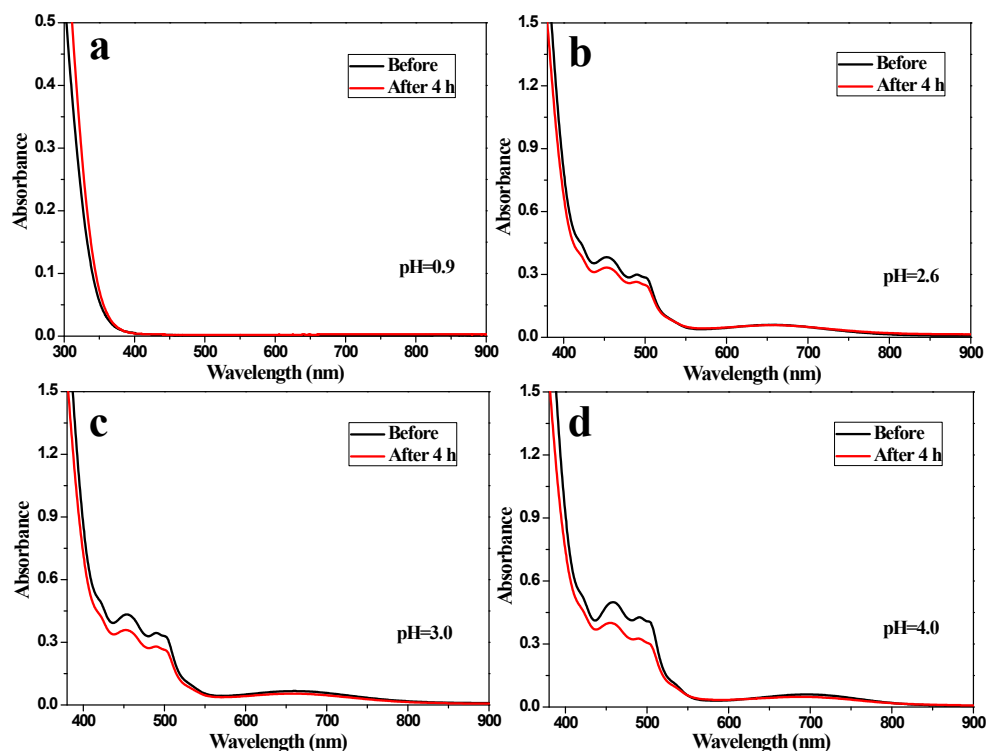


Fig. S11 UV-vis spectra before the reaction (black) and after the reaction (red), conditions: LED lamp ($\lambda=420$ nm), BiVO_4 (50 mg), NaIO_3 (5 mM) and complex **2** (500 μM), acetate buffer (pH 4.0, 0.2 M); total reaction volume 15 mL; vigorous agitation using a magnetic stirrer. The solutions are filtered before spectrum measurement.

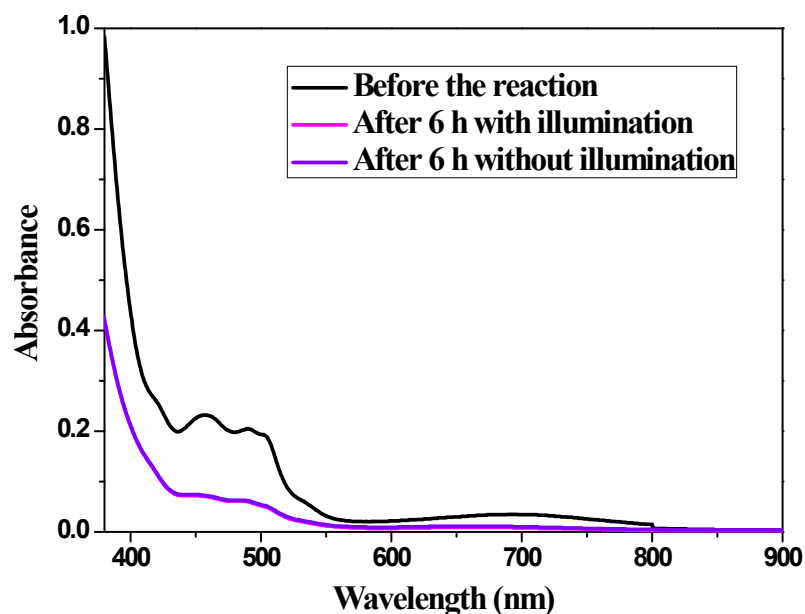


Fig. S12 UV-vis spectra before the reaction (black), after 6 h reaction with illumination (magenta) and without illumination (violet), conditions: LED lamp ($\lambda=420$ nm), BiVO_4 (50 mg), NaIO_3 (5 mM) and complex **2** (250 μM), acetate buffer (pH 4.0, 0.2 M); total reaction volume 15 mL; vigorous agitation using a magnetic stirrer. The solutions are filtered before spectrum measurement.

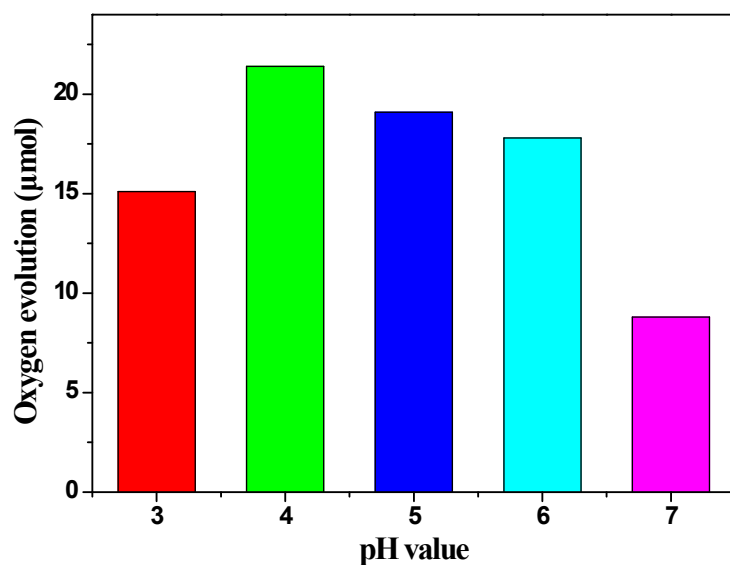


Fig. S13 Photocatalytic oxygen evolution with the artificial photosynthetic system composed of BiVO_4 (50 mg) and Fe complex **2** (50 μM) in acetate buffer (0.2 M) containing NaIO_3 (5 mM) as a function of pH under visible light irradiation ($\lambda = 420 \text{ nm}$), reaction time is 3 h.

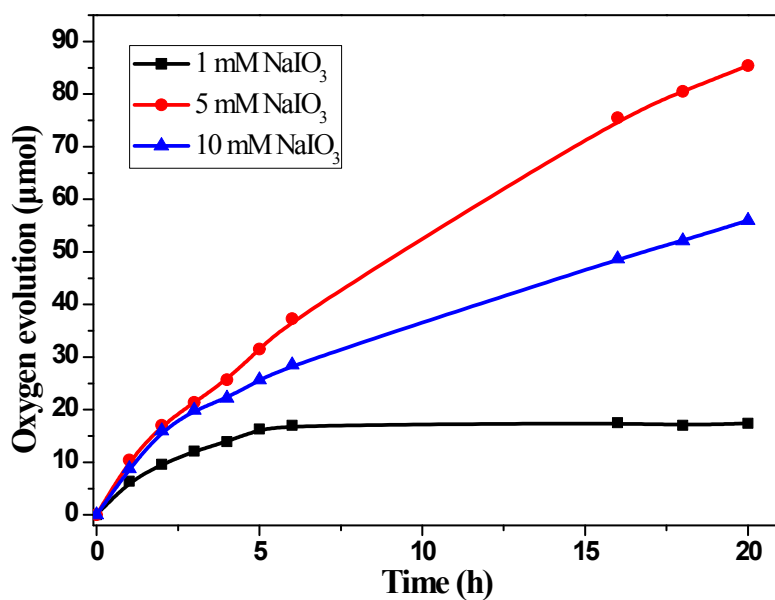


Fig. S14 Photocatalytic oxygen evolution with the photocatalytic system composed of BiVO_4 (50 mg) and complex **2** (50 μM) in acetate buffer (pH 4.0, 0.2 M) containing different NaIO_3 concentrations under visible light irradiation ($\lambda = 420 \text{ nm}$).

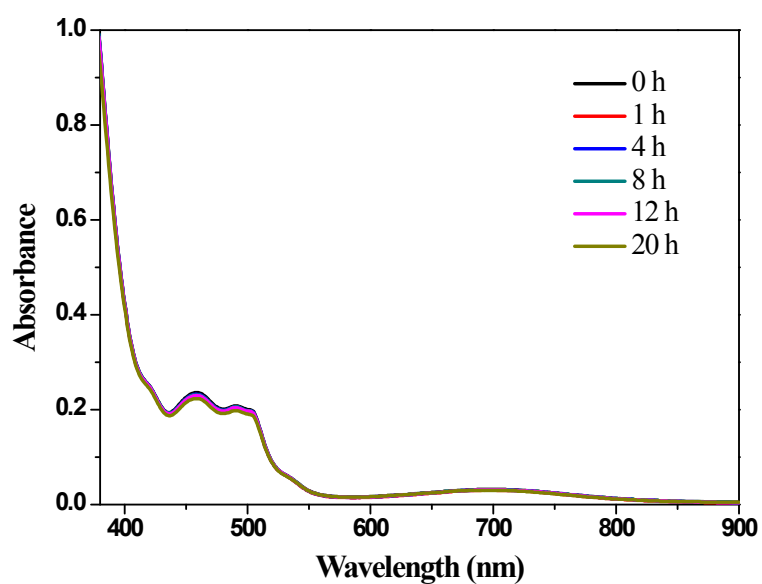


Fig. S15 Time-dependent UV-vis spectra of 250 μM **2** in acetate buffer (pH 4.0, 0.2 M).

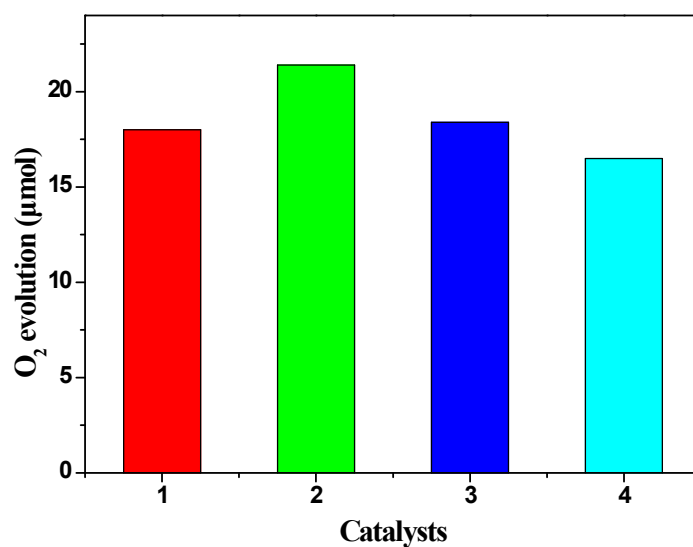


Fig. S16 Photocatalytic oxygen evolution with the artificial photosynthetic system composed of BiVO_4 (50 mg) and Fe complex **1** (100 μM), **2** (50 μM), **3** (100 μM), **4** (100 μM) in acetate buffer (0.2 M, pH 4.0) containing NaIO_3 (5 mM) under visible light irradiation ($\lambda = 420 \text{ nm}$), reaction time is 3 h.

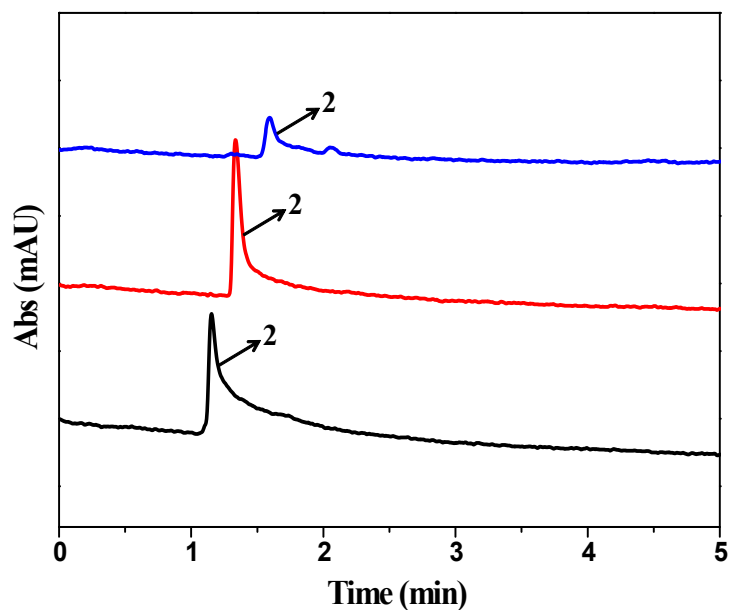


Fig. S17 An electropherogram for **2** (250 μM). Black line: 250 μM of **2** in a 20 mM acetate buffer (pH = 4.0). Red line: 250 μM of **2** in a 20 mM acetate buffer (pH = 4.0) containing NaIO_3 (10.0 mM) and 50 mg BiVO_4 (filter removal before detection), before illumination. Blue line: 250 μM of **2** in a 20 mM acetate buffer (pH = 4.0) containing NaIO_3 (10.0 mM) and 50 mg BiVO_4 (filter removal before detection) after 3 h of illumination. Experimental conditions for capillary electrophoresis: Fused-silica capillaries (75 μm i.d., 365 μm o.d., Hebei Yongnian Factory, China) with total length of 50.2 cm and effective length of 10 cm were used. The detection wavelength was set at 214 nm. The running buffer for CE separation was 20 mM sodium borate buffer (pH 10.0). The separation voltage was set at -20 kV. The sample was injected into the capillary (0.5 psi, 3 s).

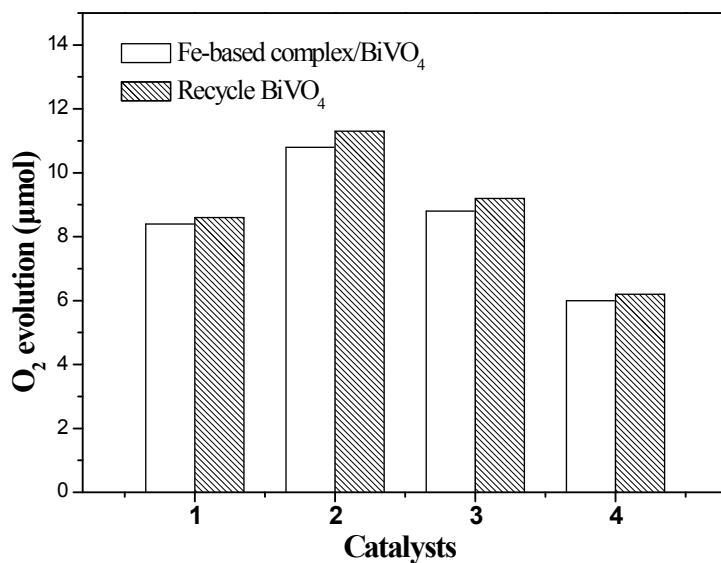


Fig. S18 Oxygen evolution activity of Fe-based complex (complex **1**, **2**, **3** and **4**) / BiVO_4 and recycle BiVO_4 after reaction.

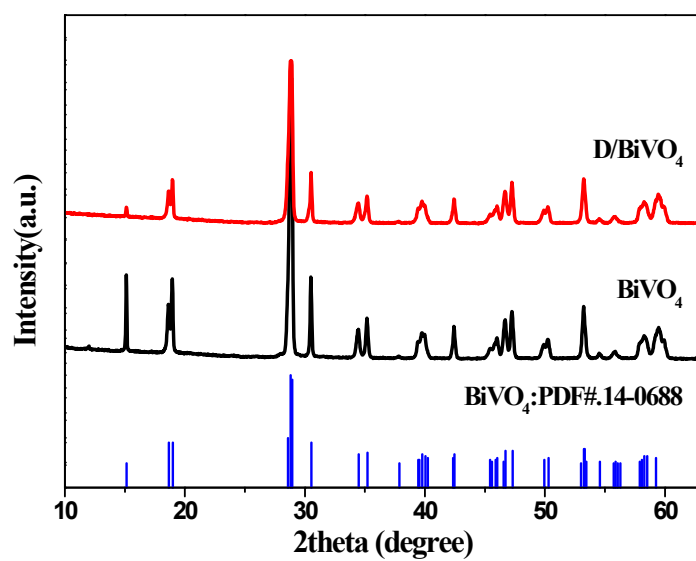


Fig. S19 The powder X-ray diffraction (XRD) spectra of pure BiVO₄ and composite D/BiVO₄.

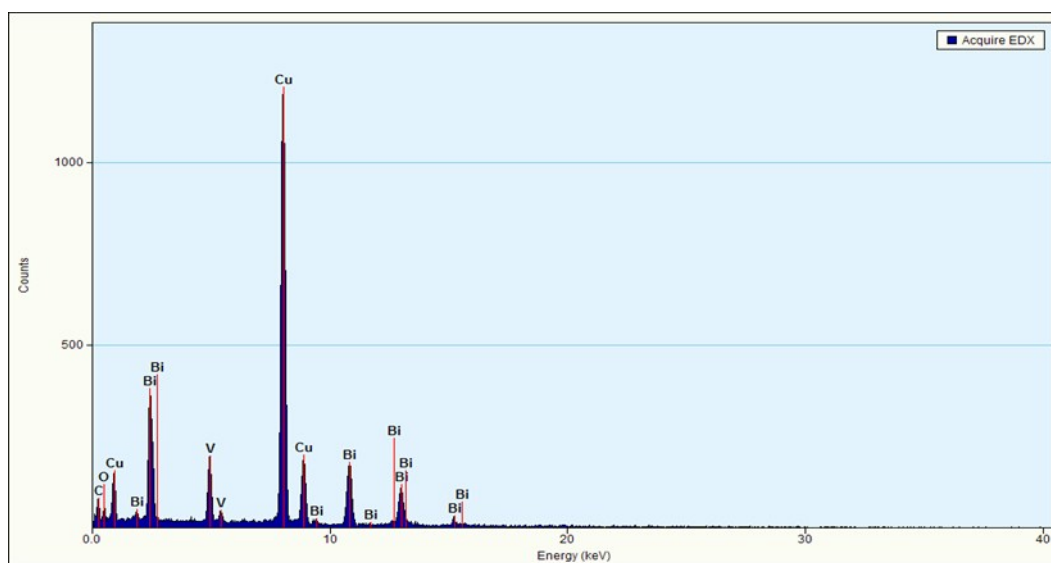


Fig. S20 EDX analysis of BiVO₄ before the reaction.

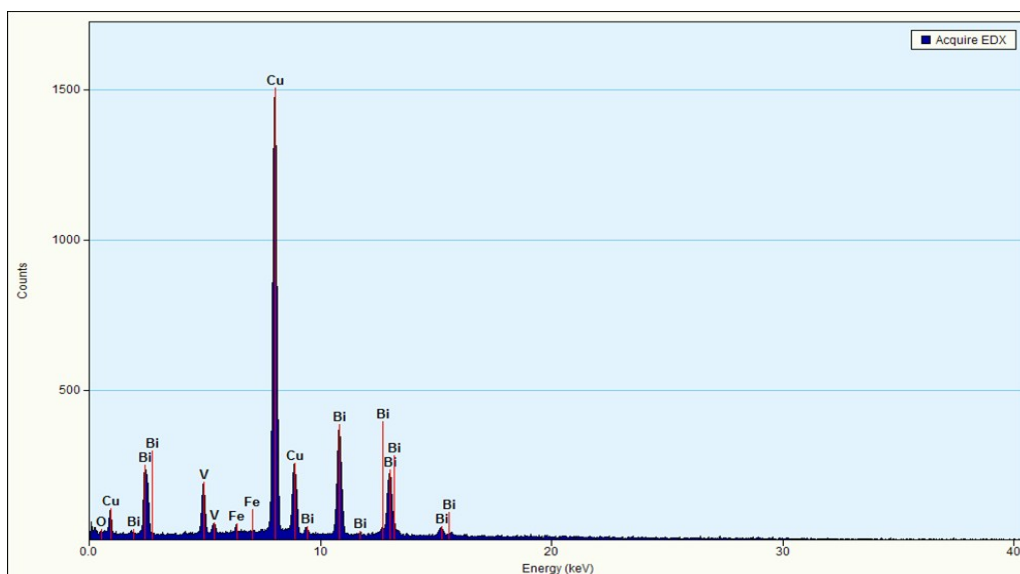


Fig. S21 EDX analysis of composite D/BiVO₄.

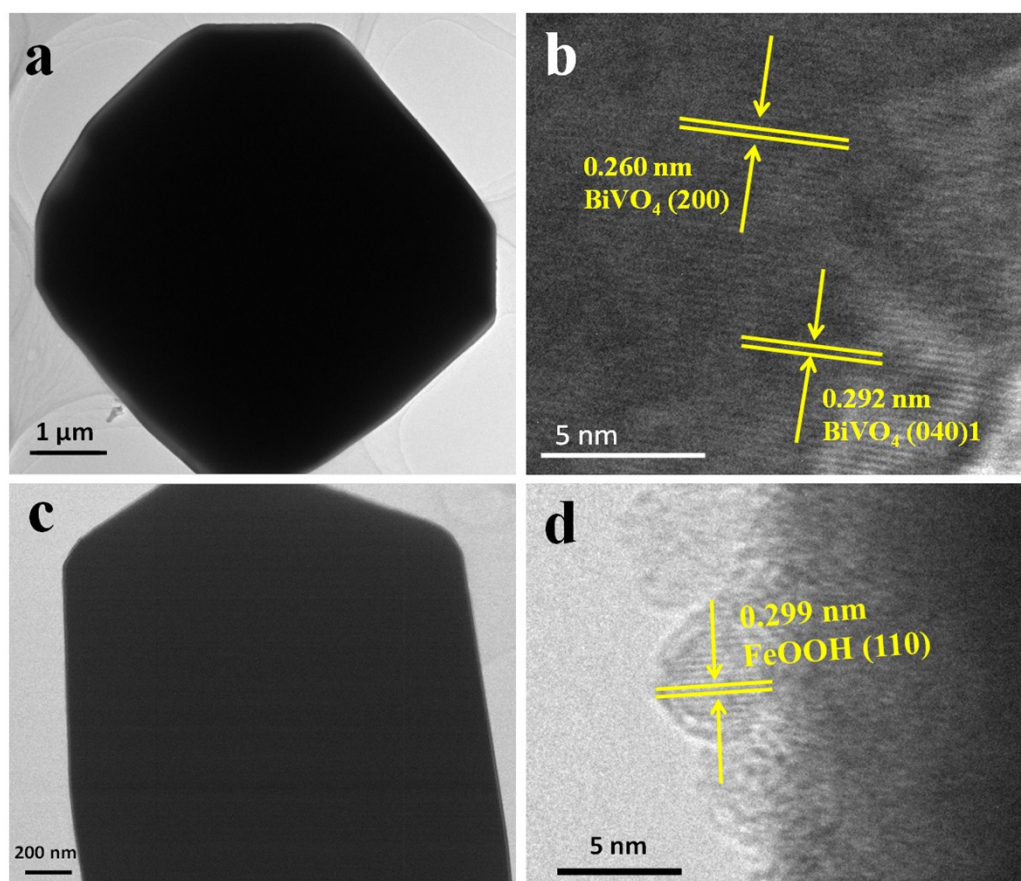


Fig. S22 Transmission electron microscopy (TEM) images of pure BiVO₄ (a) and composite D/BiVO₄ (c). High-resolution transmission electron microscopy (HRTEM) images of pure BiVO₄ (b) and composite D/BiVO₄ (d).

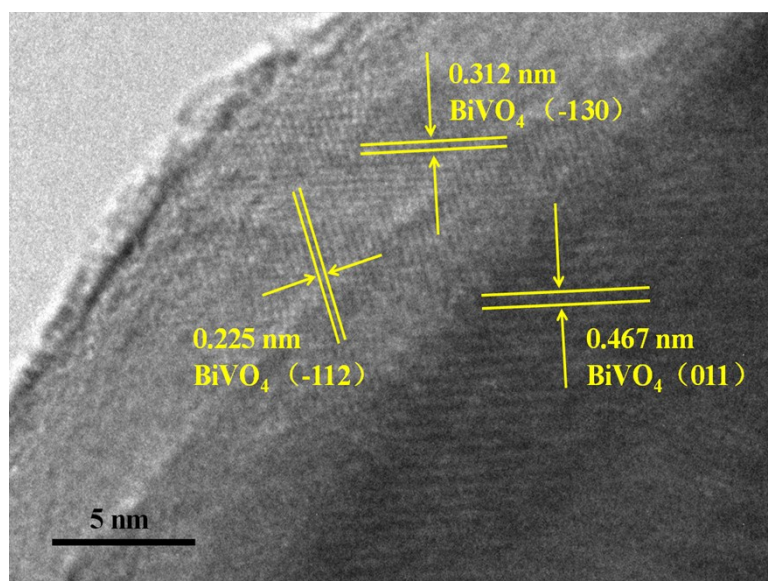


Fig. S23 High-resolution transmission electron microscopy (HRTEM) images of composite D/BiVO₄.

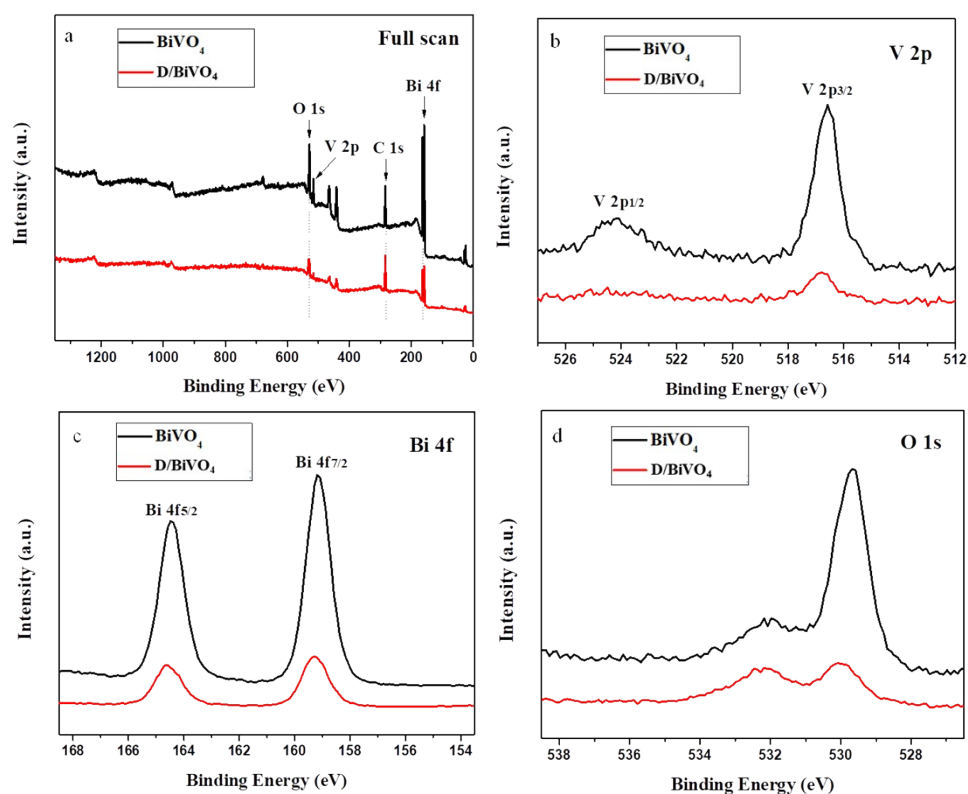


Fig. S24 The full scan of X-ray photoelectron spectroscopy (XPS) spectra of pure BiVO₄, recovered BiVO₄ (D/BiVO₄) and [Fe₂(TPA)₂(μ-O)Cl₂]Cl₂.

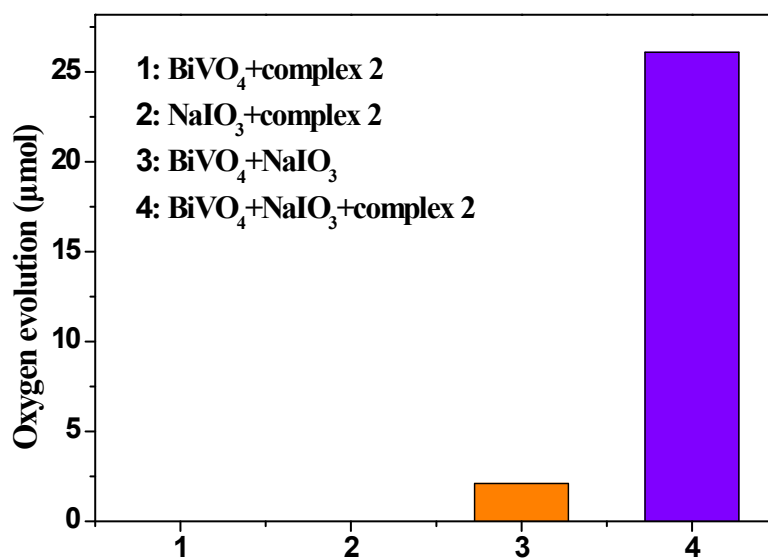


Fig. S25 The amount of oxygen evolution in the photocatalytic system. 1: 50.0 mg BiVO₄, 25 μmol complex 2; 2: 5.0 mM NaIO₃, 25 μmol complex 2; 3: 50.0 mg BiVO₄, 5.0 mM NaIO₃; 4: 50.0 mg BiVO₄, 5.0 mM NaIO₃, 25 μmol complex 2, in acetate buffer (pH 4.0), reaction time is 3 h.

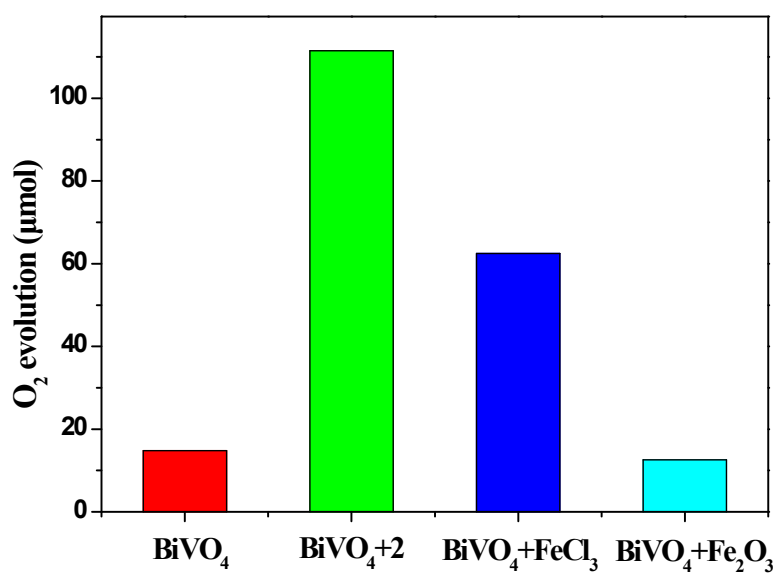


Fig. S26 The amount of oxygen evolution in the photocatalytic system using different iron sources, reaction time is 20 h. Conditions: 100 mW/cm² under illumination at 420 nm; keep the same cocatalyst concentration (25 μM), 50.0 mg BiVO₄, 10.0 mM NaIO₃;

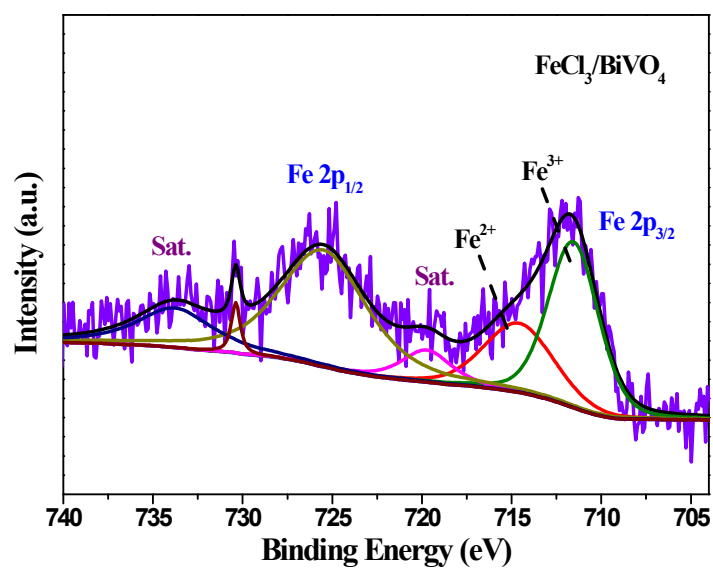


Fig. S27 The Fe 2p of X-ray photoelectron spectroscopy (XPS) spectra of recovered FeCl₃/BiVO₄ after water oxidation.

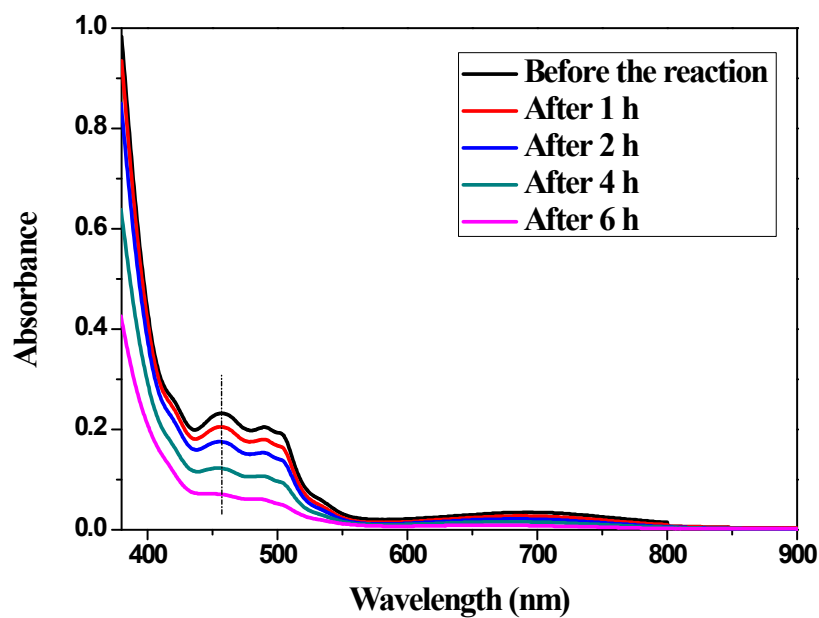


Fig. S28 Decomposition of complex 2 (250 μM) during the reaction monitored by UV-vis spectra.

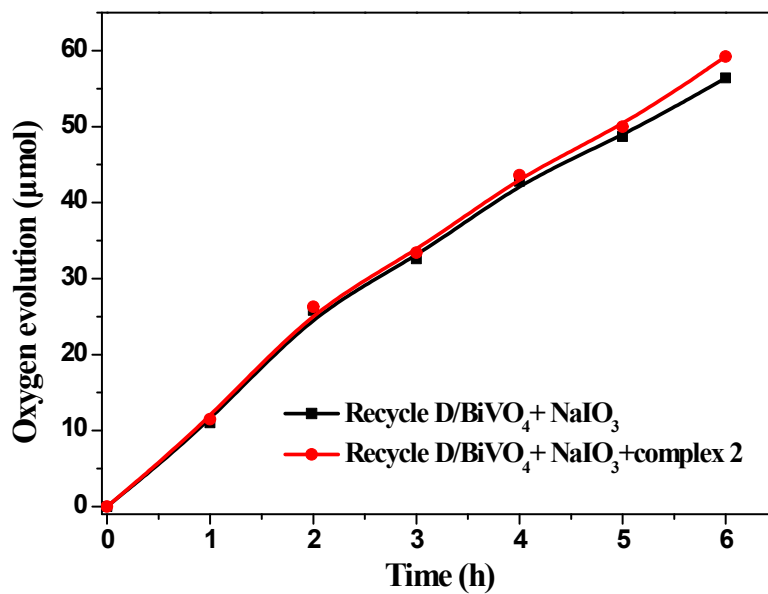


Fig. S29 Kinetics of oxygen evolution in the photocatalytic system of recycle D/BiVO₄ (without complex **2**) and D/BiVO₄ (with 25μM complex **2**) in acetate buffer (pH 4.0) containing NaIO₃ (5 mM) and BiVO₄ (50 mg).

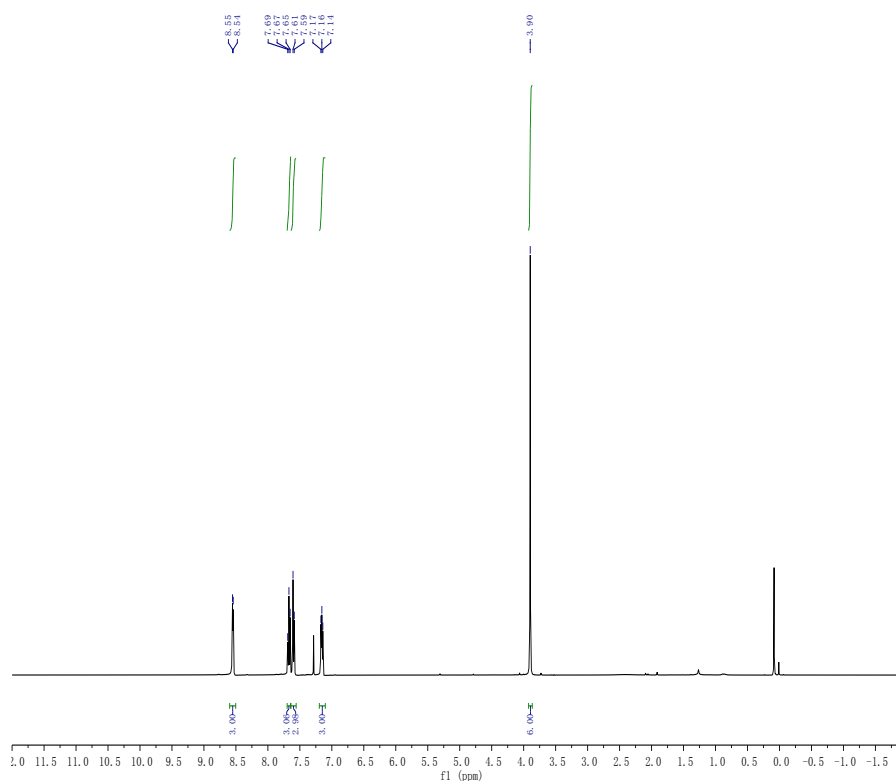


Fig. S30 ¹H NMR of TPA, ¹H NMR (400 MHz, CDCl₃) δ 8.55 (d, J = 4.6 Hz, 3H), 7.67 (t, J = 7.6 Hz, 3H), 7.60 (d, J = 7.7 Hz, 3H), 7.20 – 7.10 (m, 3H), 3.90 (s, 6H).

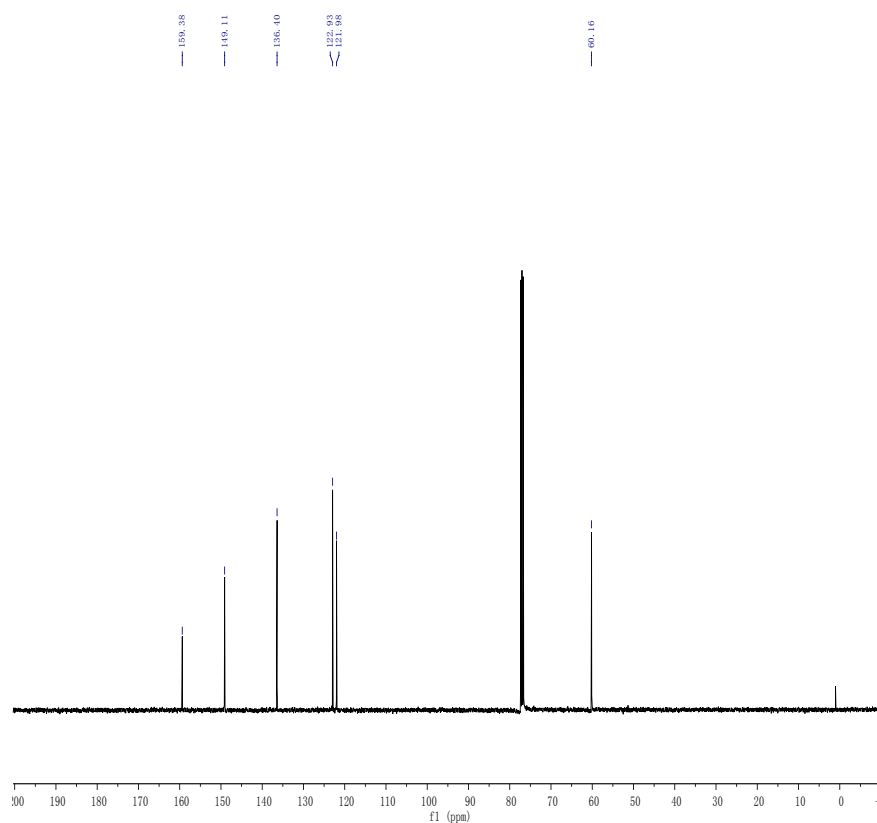


Fig. S31 ^{13}C NMR of TPA, ^{13}C NMR (101 MHz, CDCl_3) δ 159.38 (s), 149.11 (s), 136.40 (s), 122.93 (s), 121.98 (s), 60.16 (s).

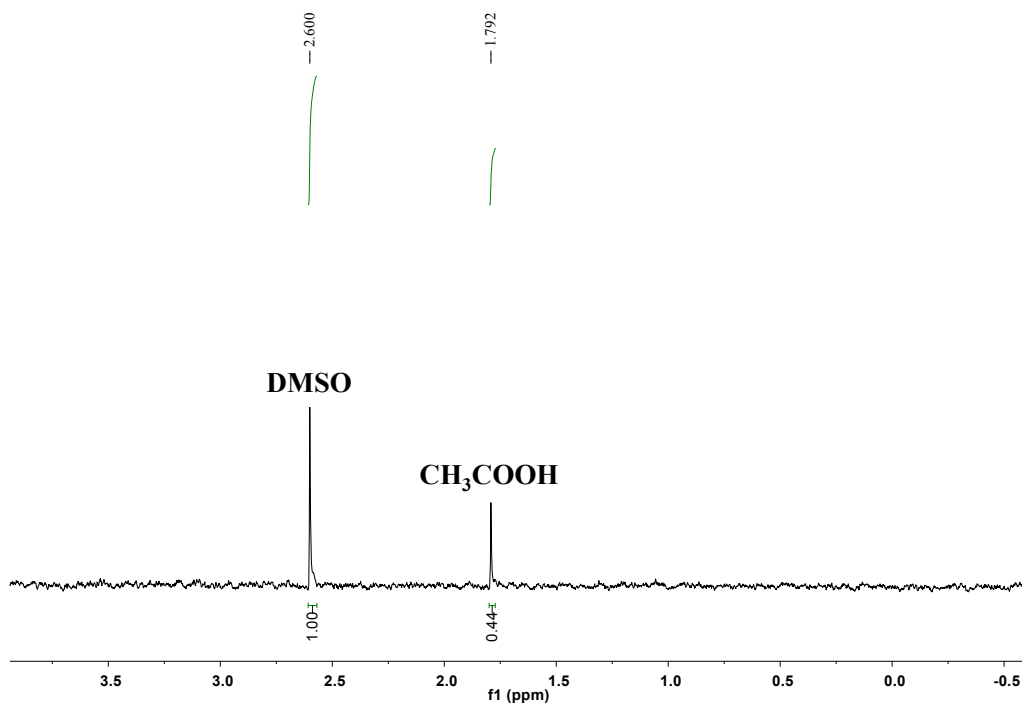


Fig. S32 The ^1H NMR spectrum of the filtered mixture of TPA (1.0 mM), BiVO_4 (50 mg), and NaIO_3 (5.0 mM) in D_2O after irradiation ($\lambda = 420$ nm) for 20 h.

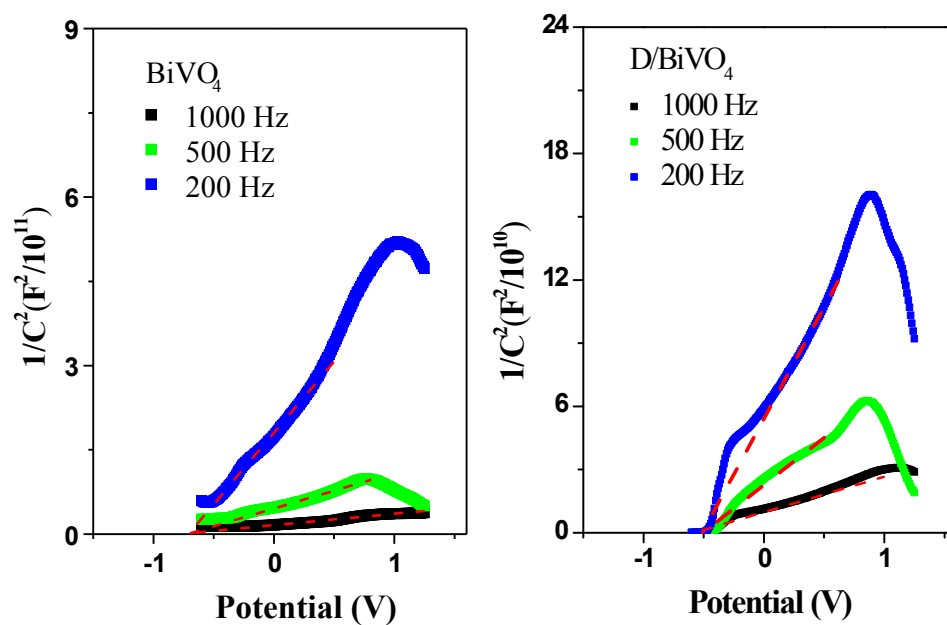


Fig. S33 Mott-Schottky plots of BiVO_4 (left) and D/BiVO_4 (right).

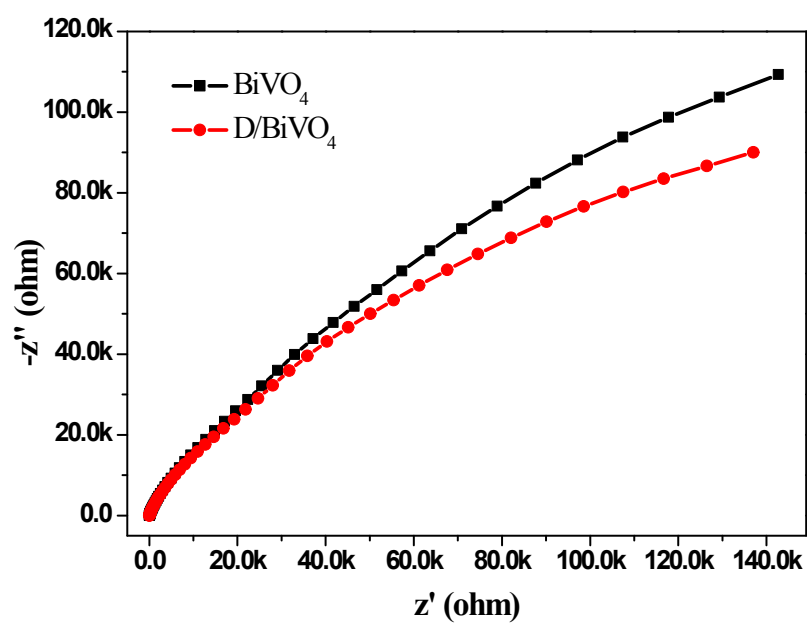


Fig. S34 Electrochemical impedance spectroscopy (EIS) for BiVO_4 and D/BiVO_4 .

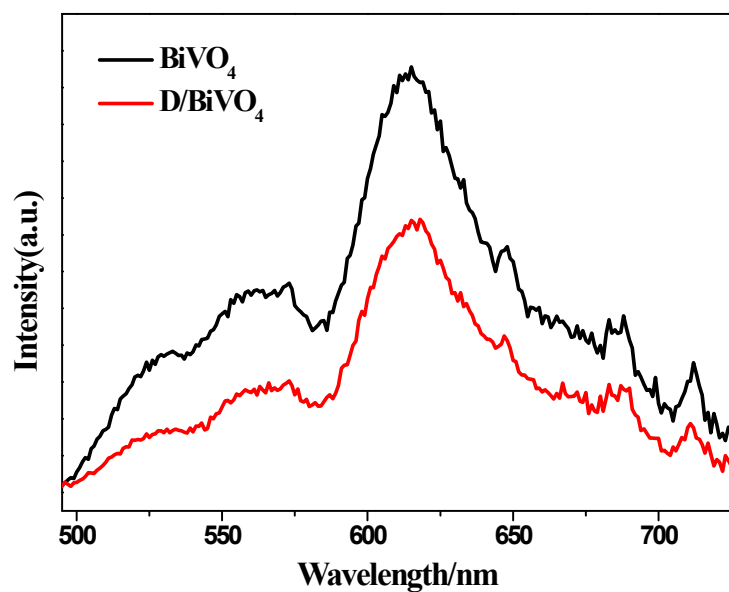


Fig. S35 PL spectra of pure BiVO_4 and D/BiVO_4 .

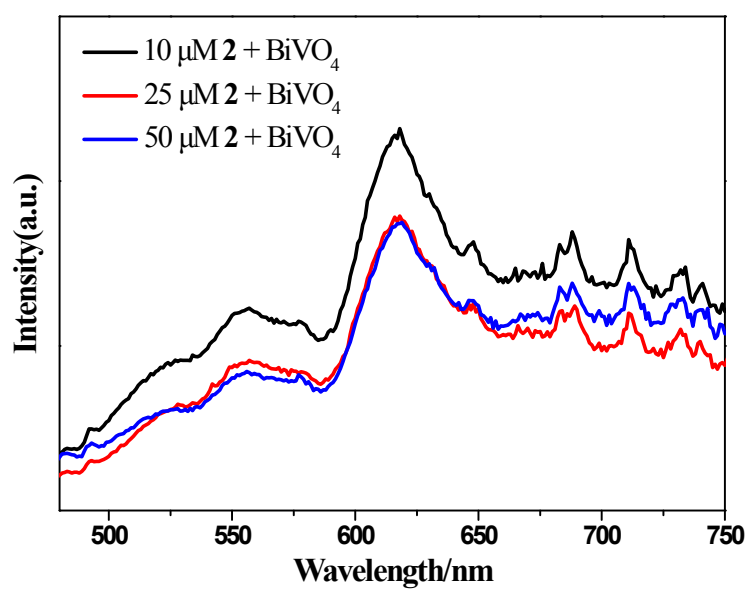


Fig. S36 Photoluminescence (PL) emission spectra of the recovered BiVO_4 prepared by the photodeposition of different concentrations (10 μM , 25 μM , 50 μM) of **2**.

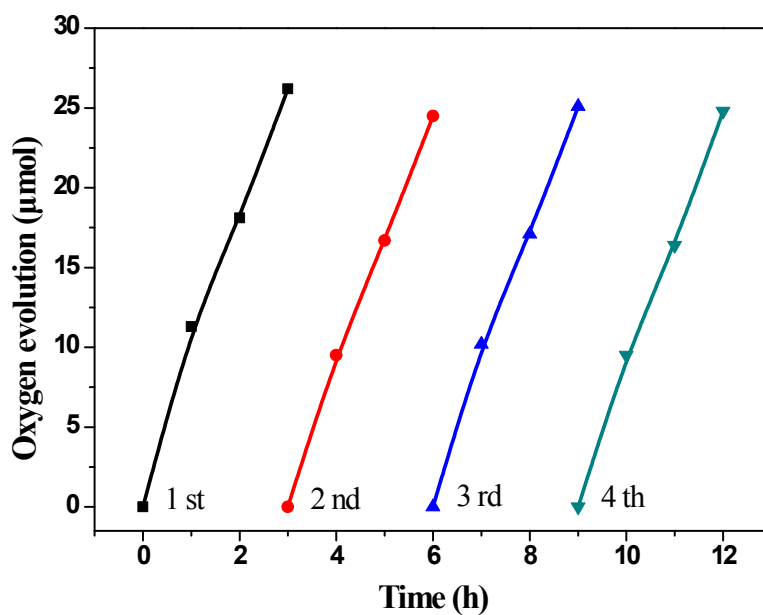


Fig. S37 Recycling photocatalytic test of composite D/BiVO₄ (50 mg) with addition of NaIO₃ in 0.2 M acetate buffer solution buffer solution at pH 4.0; all reaction solutions were irradiated by LEDs ($\lambda = 420$ nm, 100 mW cm⁻²); total reaction volume 15 mL; vigorous agitation using a magnetic stirrer.

Table S1 A comparison of water oxidation performance of different iron complexes under optimal conditions.^a

Cocatalyst	Concentration (μ M)	O ₂ evolution rate (μ mol h ⁻¹)
-	0	1.1
1	50	8.4
2	25	10.8
3	50	8.8
4	50	6.0

^aConditions: BiVO₄ (50 mg), NaIO₃ (5 mM), acetate buffer (pH 4.0, 0.2 M); keep the same iron concentration (50 μ M); reaction time is 1 h; all reaction systems were irradiated by LED lamp ($\lambda = 420$ nm).

Table S2. Water oxidation catalyzed by different catalytic systems.

Description	Approach	Time/h	n(O ₂)/μmol	Stability of molecular catalyst	Ref.
2 /BiVO ₄	Photocatalysis	2	17.8	Decomposed into FeOOH	This work
FeP /WO ₃	Photoelectrochemical	2	3.7±0.4	Stable	5

Table S3 Concentration of Fe detected by ICP-AES.

Samples ^a	Concentration of complex 2 (μM)	Concentration of Fe (mg/L) ^b
1	10	2.05
2	25	3.09
3	50	6.60

^a The method for the preparation of samples: The acetate buffer solution containing complex **2**, NaIO₃ and BiVO₄ was illuminated 20 h; conditions: 50 mg BiVO₄, 5 mM NaIO₃, and 420 nm LED lamp, pH 4.0 acetate buffer; total reaction volume 15 mL; vigorous agitation using a magnetic stirrer. The recycled BiVO₄ was washed with ultrapure water and dried under vacuum at 40 °C for 24 hours. Then, 100 mg recycled BiVO₄ was dissolved in 10 mL aqueous hydrochloric acid (4 M) for the ICP-AES analysis. ^bThe concentration of Fe represents the thickness of FeOOH on the surface of BiVO₄.

References

1. Y. Liu, R. Xiang, X. Du, Y. Ding and B. Ma, *Chem. Commun.*, 2014, **50**, 12779.
2. Y. Hitomi, K. Hiramatsu, K. Arakawa, T. Takeyasu, M. Hata and M. Kodera, *Dalton Trans.*, 2013, **42**, 12878.
3. Q. Li, T. A. van den Berg, B. L. Feringa and G. Roelfes, *Dalton Trans.*, 2010, **39**, 8012.
4. M. Lubben, E. C. Wilkinson, B. Feringa, and L. Que, Jr., *Angew. Chem., Int. Ed.*, 1995, **34**, 1512.
5. T. E. Rosser, M. A. Gross, Y.-H. Lai and E. Reisner, *Chem. Sci.*, 2016, 7, 4024.